Small-Angle Neutron Scattering Study on Charged Gels in Deformed State

Mitsuhiro Shibayama,* Kazuki Kawakubo, and Fumiyoshi Ikkai

Department of Polymer Science and Engineering, Kyoto Institute of Technology, Matsugasaki, Sakyo-ku, Kyoto 606-8585, Japan

Masayuki Imai

Institute for Solid State Physics, The University of Tokyo, Tokai, Ibaragi 319-11, Japan

Received September 23, 1997; Revised Manuscript Received February 7, 1998

ABSTRACT: The structure of weakly charged temperature sensitive gels has been investigated in deformed state by means of small-angle neutron scattering (SANS). At low temperatures where the gel is in a good solvent, the scattered intensity pattern was isotropic even for deformed gels. When the temperature was raised to 42 °C, the so-called butterfly pattern, i.e., a prolate-shaped scattered intensity pattern with respect to the stretching direction, appeared in the deformed gels. With a further increase in temperature to 46 °C, a scattering maximum was observed. In the case of undeformed gel, the scattering pattern had a circular maximum with $q = q_m$, where q is the magnitude of the scattering vector and q_m is the q value at the scattering maximum. On the other hand, the scattering pattern became oblate for the deformed gel, i.e., $q_{m,y} < q_{m,x}$, where the subscripts y and x indicate the stretching and perpendicular directions, respectively. These changes of the SANS intensity patterns are discussed by decomposing it into the thermal fluctuations and the static inhomogeneities.

Introduction

It has recently been recognized that the concentration fluctuations in polymer gels consist of thermal fluctuations and static (spatial) inhomogeneities.[1−8] The former are the dynamic fluctuations similar to those present in semidilute polymer solutions. However, the latter are characteristic of gels and are originated from cross-linking. The contribution of the static inhomogeneities is enhanced by swelling or stretching the gel. This is due to the fact that by deformation (e.g., swelling or stretching) a coarsely cross-linked region deforms more than a densely cross-linked region, resulting in enhancement of the concentration difference between the two regions. This kind of concept was introduced by Bastide and Leibler[1] and then experimentally verified by Rouf et al.[5] and Mendes et al.[9] The presence of static inhomogeneities in gels is demonstrated as so-called butterfly pattern. When a gel is uniaxially stretched, an increase in the scattered intensity appears in the stretching direction. Since this elliptic contour pattern is opposite to that theoretically predicted on the basis of thermal fluctuations, this pattern is sometimes called "abnormal butterfly pattern".[10] The abnormal butterfly pattern has been interpreted with a concept of frozen (or quenched) inhomogeneities, which becomes significant as the gel is deformed.[11]

When charges are introduced to a neutral polymer gel, the swelling ratio becomes larger. If the volume of the gel is fixed during ionization or, in other words, if the gel is isolated from the reservoir during ionization, the static inhomogeneities are suppressed due to strong Donnan potential generated in the gel.[12,13] However, the situation changes completely when the solvent becomes poor to the network polymer. Because of antagonistic move of the chains, i.e., homogeneization by electroneutrality and segregation by solvent−polymer immiscibility, the polymer gel undergoes a microphase separation.[14,15] This phenomenon was first predicted by Borue and Erukhimovich for polyelectrolyte solutions in a poor solvent.[16] Experimentally, Schosseler et al.[17] observed the presence of scattering maximum in the structure factor of partially neutralized poly(acrylic acid) gels by small-angle neutron scattering (SANS). Shibayama et al. reported presence of a strong scattering maximum in SANS appeared for weakly charged polymer gels of poly(*N*-isopropylacrylamide-*co*-acrylic acid) (NIPA/AAc) gels[14] and solutions.[18] The scattering maximum appeared around $q = 0.02$ Å^{-1} and increased with increasing temperature, where q is the magnitude of the scattering vector. The change of the scattered intensity was more than 100-fold by changing temperature from 25 to 50 °C. This peak is due to the competition of the electroneutrality and immiscibility in the gel and indicates an occurrence of microphase separation. Recently, a more elaborate scattering theory for weakly charged gels was proposed by Rabin and Panyukov[19] of which the relevancy has been discussed by Shibayama et al.[20]

A study of the structure factor of weakly charged polyelectrolyte gels under uniaxial stretching was carried out by Mendes et al.[21] They observed disappearance of a butterfly pattern and an intensity increase in the perpendicular direction than in the parallel direction by introducing ions to the gel network. However, it has not been elucidated whether the origin of the scattering maximum is thermal fluctuations or static (quenched) inhomogeneities. In order to answer this question, we carried out a SANS experiment on weakly charged polymer gels in deformed state, of which the results are reported in this paper. Temperature-sensitive gels were chosen due to easy control of the miscibility between polymer and solvent just by temperature. However, the following problem had to be solved to conduct the SANS

* To whom correspondence should be addressed.

S0024-9297(97)01411-3 CCC: $15.00
Published on Web 04/03/1998

experiment on deformed gels. Since gels are very fragile, deformation of gels is very difficult. Particularly in the case of charged gels, this is a formidable problem due to a high swelling ratio of charged gels compared to uncharged gels. A unique idea was proposed by Geissler et al., who employed a mold having an elliptical hole and let a shrunken gel swell anisotropically.[22] This method was successful for uncharged gels. In this study, however, since we aimed to change the deformation ratio many times, employment of elliptical holes was not relevant. Instead, we designed a deformation chamber for gels. The concept of the deformation lies in an idea that a gel embedded in a rubber deforms as the rubber deforms. This allows us to deform a gel with a desired amount of deformation without breaking the gel. Here, we first report the structure factor of weakly charged gels as a function of temperature and of the degree of stretching. Then, we analyze the structure of these gels by decomposing the structure factor into two contributions from thermal fluctuations and static inhomogeneities.

Theoretical Background

The structure factor for a deformed gel is predicted by Onuki, who introduced frozen inhomogeneities in addition to thermal fluctuations.[4] This theory was successfully employed by Mendes et al.[9] in order to interpret their anisotropic scattered intensity patterns of poly(dimethylsiloxane). In the case of weakly charged gels in deformed state, a theory proposed by Rabin and Panyukov,[19] hereafter we call the RP theory, is available at this stage. This theory is an extension of their theory on neutral gels (referred as the Panyukov−Rabin theory)[6] to weakly charged gels. The Panyukov−Rabin theory is based on the assumption of instantaneously cross-linked polymer network in which each polymer chain behaves as a Gaussian chain with an excluded volume. The theory allows one to take account of two parameter sets, i.e., one at preparation and the other at observation. The structure factor consists of a contribution from thermal fluctuations, $G(q)$, and that from static density inhomogeneities, $C(q)$

$$S(q) = G(q) + C(q) \tag{1}$$

$$G(q) = \frac{\phi N g(q)}{1 + w(q)g(q)} \tag{2}$$

$$C(q) = \frac{\phi N}{[1 + w(q)g(q)]^2(1 + Q^2)^2} \times \left[6 + \frac{9}{w_0(q) - 1 + \{(Q_y^2\lambda_y^2 + Q_x^2\lambda_x^2)\}(\phi_0/\phi)^{2/3}\phi_0^{-1/4}/2}\right] \tag{3}$$

where N denotes the average degree of polymerization between cross-linking points. ϕ and ϕ_0 are the polymer volume fractions at observation and at preparation, respectively. Note that we defined $G(q)$ and $C(q)$ to be dimensionless functions in order to take an advantage of independence of the choice of the segment volume a^3, which appears in the original RP theory. Q is defined as the dimensionless wave vector by

$$Q = aN^{1/2}q \tag{4}$$

where a is the segment length, and Q_y and Q_x are the projections of the wave vector, along and normal to the stretching direction, respectively. It should be noted that $C(q)$ and $G(q)$ are coupled with the function $g(q)$, which is given by

$$g(q) = \frac{1}{Q^2/2 + (4Q^2)^{-1} + 1} + \frac{2Q^2\phi^{2/3}\phi_0^{-12/5}}{(1 + Q^2)^2(Q_y^2\lambda_y^2 + Q_x^2\lambda_x^2)} \tag{5}$$

Therefore, eq 1 can be written in the following form:

$$S(q) = G(q)\left\{1 + \frac{G(q)}{\phi N g^2(q)}\frac{1}{(1 + Q^2)^2} \times \left[6 + \frac{9}{w_0(q) - 1 + \{(Q_y^2\lambda_y^2 + Q_x^2\lambda_x^2)\}(\phi_0/\phi)^{2/3}\phi_0^{-1/4}/2}\right]\right\} \tag{6}$$

The characteristic feature of the RP theory is the fact that the dimensionless quantities $w(q)$ and $w_0(q)$ represent the effective second virial coefficients in the final state and in the state of preparation, respectively, and are q-dependent since the electrostatic interaction is a long-range interaction. Those are given by[19]

$$w(q) = (1 - 2\chi + \phi)\phi N + \frac{\hat{l}_B f^2 \phi N^2}{Q^2 + \hat{l}_B f \phi N} \tag{7}$$

$$w_0(q) = \phi_0^{5/4}N + \frac{\hat{l}_B f_0^2 \phi_0^{5/4} N^2}{(Q_y^2\lambda_y^2 + Q_x^2\lambda_x^2)(\phi_0/\phi)^{2/3} + \hat{l}_B f_0 \phi_0^{5/4} N} \tag{8}$$

where χ is the Flory interaction parameter at the state of measurement and $\hat{l}_B$ ($\equiv l_B/a$) is the dimensionless Bjerrum length l_B ($\approx$ 7 Å in water at 25 °C). It is assumed that the gel was prepared under good solvent conditions. Thus, $S(q)$ is expressed as a function of two sets of parameters in the preparation state (w_0, ϕ_0) and under conditions of observation (w, ϕ). The applicability of the RP theory has been discussed elsewhere.[20]

Experimental Section

1. Sample Preparation. A slab gel of poly(*N*-isopropylacrylamide-*co*-acrylic acid) (NIPA/AAc) was prepared in deuterated water by redox polymerization. NIPA monomers, kindly supplied by Kohjin Chem. Co., Tokyo, Japan, were recrystallized before use. The monomer concentrations were 668 mM (NIPA) and 32 mM (AAc). Cross-linking was attained by copolymerizing 8.6 mM of *N*,*N*′-methylenebis(acrylamide) (BIS). A pregel solution containing NIPA, AAc, BIS, and ammonium persulfate was degassed before polymerization. The reaction was initiated by adding 24 mM of *N*,*N*,*N*′,*N*′-teteramethylethylenediamine (accelerator) to the pregel solution in the reactor batch, made of a Petri dish with a 3 mm-glass spacer. The polymerization temperature was 20 °C. Thus a prepared gel, 3 mm thick, was used without further purification. The degree of ionization at preparation, f_0, was estimated to be 0.0457.

2. Sample Deformation. A disk-shape of gel was punched out from the slab and was transferred to a silicon rubber mold. The mold, of 3 mm thick and of square shape, has a 30 mm diameter hole in the center as shown in Figure 1A. The mounted gel in the mold (b) was sealed in a thermostated chamber made of brass (c) with a pair of quartz windows (d). The gel was deformed by compressing the rubber from both sides (along the x direction) by screws (e). Figure 1B shows

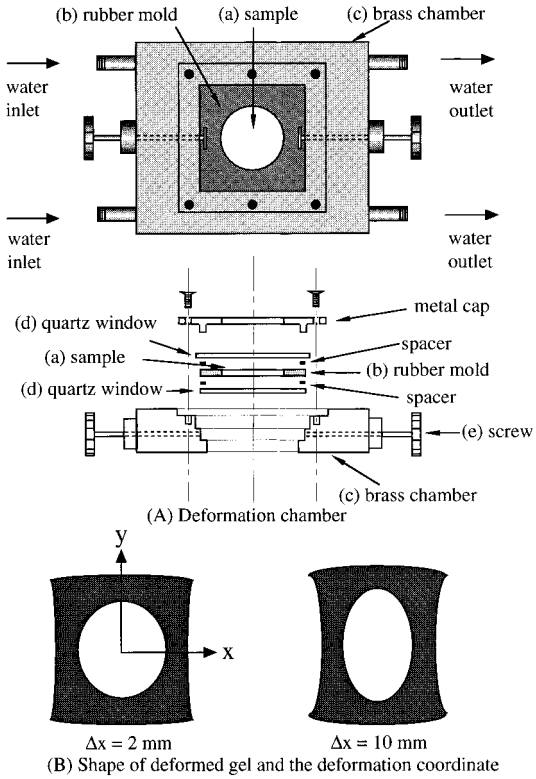

Figure 1. (A) Deformation chamber and (B) shape of deformed gels and the deformation coordinate.

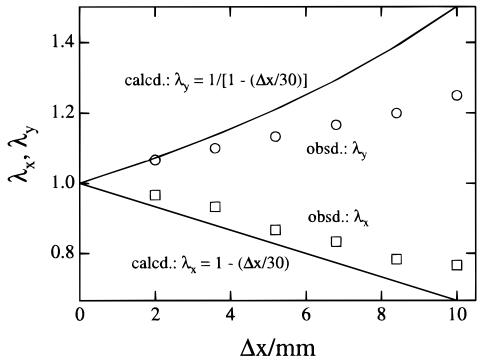

Figure 2. Deformation ratios, λ_x and λ_y as a function of the deformation of the silicon rubber, Δx.

the shape of the gel compressed by $\Delta x = 2$ mm (left) and by $\Delta x = 10$ mm (right). The deformation coordinate is also shown in the figure. In the case of $\Delta x = 10$ mm, the gel is stretched in the y direction by $\lambda_y = 1.25$ and compressed in the x direction by $\lambda_x = 0.77$, where λ_y and λ_x are the deformation ratios along the stretching and perpendicular directions, respectively.

Figure 2 shows the deformation ratios, λ_y and λ_x as a function of the deformation of the rubber, Δx. The solid lines are the calculated deformation ratios, which are estimated by

$$\lambda_x \equiv \frac{30 - \Delta x}{30} = 1 - \frac{\Delta x}{30} \tag{9}$$

$$\lambda_y \equiv \frac{1}{\lambda_x} = \frac{1}{1 - (\Delta x/30)} \tag{10}$$

Note that the sample was deformed two dimensionally by keeping the thickness. Therefore, the calculated λ_y is given by $1/\lambda_x$ and not by $1/\sqrt{\lambda_x}$ (uniaxial stretching of a three dimensional object), where no volume change is assumed by deformation. Due to the indirect deformation via the silicon rubber mold, a noticeable deviation from the calculated deformation is clearly seen even in the x direction. This is due to compression of the rubber. Therefore, in the following, the analysis will be conducted as a function of the observed deformation ratios.

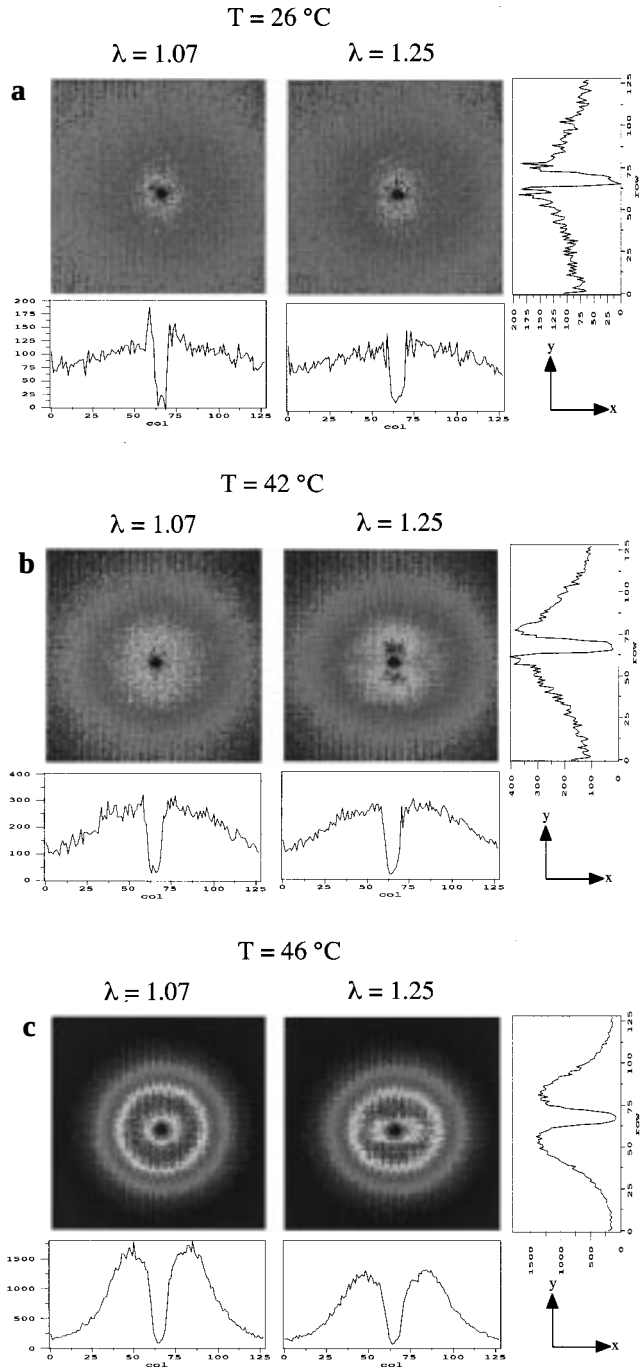

Figure 3. Two-dimensional SANS intensity profiles of NIPA/AAc gels at (a) 26, (b) 42, and (c) 46 °C. The figures on the left show the SANS patterns for gels with low stretching ratio, i.e., $\lambda = 1.07$, along the y (stretching) direction, and the right corresponds to those for highly deformed gels with $\lambda = 1.25$. The scattered intensity functions along the equator (col; column) and along the meridian (row) are also shown below or on the right of the SANS intensity profiles with the intensity scales (in counts of neutrons per 1 h).

3. SANS Experiment. A uniformly deformed gel in the deformation chamber was investigated by SANS. The temperature of the chamber was controlled by circulating water with the precision of ±0.5 °C (See Figure 1A). The SANS experiment was carried out at the SANS-U, The Solid State Institute, The University of Tokyo, Tokai, Ibaragi, Japan. A cold neutron flux with the wavelength of 7 Å was used as an

incident beam. The diameter of the incident neutron beam was 5 mm, which is much smaller than the size of the gel. The sample to detector distance was 4 m. The beam stop was 40 mm o.d. The gel sample was exposed by the neutron beam for 1−2 h depending on the scattered intensity. SANS experiments on the gels were carried out as a function of both temperature (26, 35, 42, 44, and 46 °C) and deformation ($\lambda \equiv \lambda_y = 1.0, 1.10, 1.13, 1.17, 1.20$, and 1.25). Circular averaging was done for undeformed gels, while a sector average was taken with the sector angle of 20° for deformed gels with respect to the equator (the x direction) and to the meridian (the y axis) in the reciprocal space, respectively, whereas a circular average was applied to undeformed gels. The averaged data were corrected for cell scattering, transmission, sample thickness, and incoherent scattering and then were scaled to the absolute intensity with a scale factor determined with the incoherent scattering of a Lupolen standard.

Results and Discussion

1. SANS Isointensity Patterns. Parts a−c of Figure 3 show the SANS intensity profiles of NIPA/AAc gels at (a) 26, (b) 42, and (c) 46 °C. The figures on the left show the two dimensional (2D) SANS patterns (upper) for gels with low stretching ratio, i.e., $\lambda = 1.07$, along the y (stretching) direction, and the right corresponds to those for highly deformed gels with $\lambda = 1.25$. Instead of a contour or a gray scale representation, the intensity profiles were obtained with a pseudo-color scale (rainbow) and then were printed with a gray scale in order to enhance the intensity contrast. For quantitative comparison, the scattered intensity functions along the equator (col; column) and along the meridian (row) are also shown below and on the right of the SANS intensity profiles with the intensity scales (in counts of neutrons per 1 h). At low temperatures including 26 °C, the SANS patterns are rather isotropic irrespective of the state of deformation. However, anisotropy starts to appear in the deformed gel at 42 °C. The scattered intensity patterns at 42 °C are similar to the so-called butterfly pattern (or more exactly the abnormal butterfly pattern). The scattered intensity contour has a lobe in the stretching direction. At 46 °C, a distinct peak appears in both undeformed and deformed gels. By deforming the gel, the scattering maximum became elliptic and q_m moves to the low q direction in the stretching direction, while the scattered intensity on the equator (i.e., along the x direction) seems to be suppressed. Though they would be very interesting, SANS measurements above 46 °C were impossible due to the limit of the detector capacity.

Figure 4 shows the variation of q_m along ($q_{m,y}$; large squares) and perpendicular directions ($q_{m,x}$; large circles) as a function of deformation, Δx. By further deformation the gel, the scattering ellipse becomes more anisotropic, giving smaller $q_{m,y}$ and larger $q_{m,x}$ for larger Δx. The solid lines with small circles and squares indicate the expected values of $q_{m,y}$ and $q_{m,x}$ on the basis of affine deformation. Since the gel undergoes two-dimensional deformation, the following relation holds for affine deformation:

$$q_{m,x} = q_{m,0}/\lambda_x \tag{11}$$

$$q_{m,y} = q_{m,0}/\lambda_y \tag{12}$$

As shown in the figure, the observed $q_{m,x}$ is well predicted by the affine deformation, while a noticeable deviation is found in $q_{m,y}$, i.e., in the stretching direction. However, it is clear that the macroscopic deformation

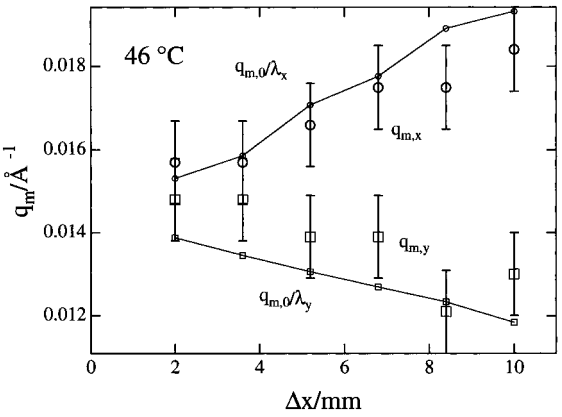

Figure 4. Changes of the scattering maximum, q_m, as a function of the deformation of the rubber, Δx. The solid lines indicate the calculated $q_{m,y}$ and $q_{m,x}$ by assuming affine deformation.

is more or less effectively transmitted to the microscopic deformation. This finding, i.e., the presence of elliptic scattering maximum, is very important. If the scattering is purely ascribed to thermal fluctuations, the maximum should be isotropic and be independent of deformation. In such a case, charged regions in the network may rearrange themselves to keep equidistance with each other to minimize the electrostatic energy irrespective of deformation. The experimental finding indicates that it does not happen in a real gel. The appearance of anisotropic scattering maximum indicates that the spatial distribution of the charged groups changes by deformation. Therefore, it can be deduced that the anisotropic scattering maximum is strongly coupled with the solidlike inhomogeneities. We will discuss this problem more quantitatively in a later section.

It should be noted here that anisotropic scattering is characteristic of gels *in poor solvent*. No distinct anisotropy in the scattering profile is seen for the gel at 26 °C. This observation is in good agreement with that by Mendes et al. for weakly charged poly(acrylic acid) gels.[21] This fact may be explained as follows: In a weakly charged gel, there are at least three contributions to the osmotic pressure, those from mixing free energy, Π_{mix}, entropy elasticity, Π_{el}, and Donnan potential (or electrostatic interactions), Π_D, i.e.[15,23,24]

$$\Pi = \Pi_{mix} + \Pi_{el} + \Pi_D \tag{13}$$

If a gel is in swelling equilibrium, $\Pi = 0$. However, for a gel of which the volume is fixed, Π is usually positive. This is easily attained, for example, by filling the gel in a container with a fixed volume, which is the case studied here. Since the square of concentration fluctuations, $|\delta\phi|^2$, are proportional to the inverse of the derivative of Π with respect to ϕ, i.e.

$$|\delta\phi|^2 \sim kT\phi/\left(\frac{\partial\Pi}{\partial\phi}\right) \tag{14}$$

a large value of $(\partial\Pi/\partial\phi)$ results in a suppression of concentration fluctuations. This corresponds to a gel at low temperatures where the solvent is good to the polymer consisting of the network. However, as the temperature is increased, Π_{mix} becomes negative and the total osmotic pressure becomes smaller or even negative. In such a case, the concentration fluctuations inherently present in the gel become apparent. This

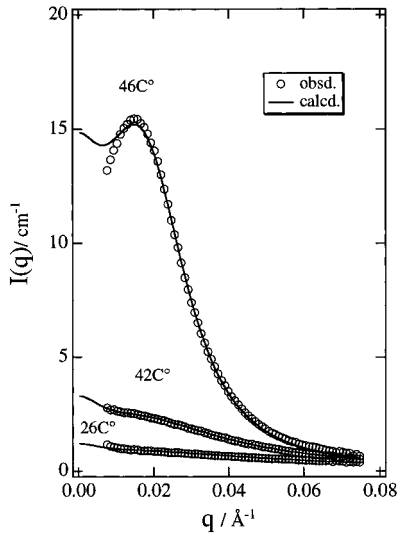

Figure 5. Circularly averaged $I(q)$'s of NIPA/AAc gels at 26, 42, and 46 °C. Results of curve fitting with eqs 1−8 are shown with solid lines. The fitted parameter sets of (χ, K) are (−0.221, 1.359), (0.322, 1.412), and (0.748, 1.021), respectively, for the gels observed at 26, 42, and 46 °C.

leads to an appearance of a butterfly pattern for a stretched gel as shown in Figure 3b. Now, we analyze the elliptic scattering patterns on the basis of the Rabin−Panyukov theory for weakly charged gels.

2. Prediction of Elliptic Scattering Pattern. A curve fitting of the SANS intensity functions was carried out on the basis of the RP theory by floating two parameters, i.e., the contrast factor, K, and χ, where

$$I(q) = KS(q) \tag{15}$$

Figure 5 shows scattered intensity functions, $I(q)$, of undeformed NIPA/AAc gel at 26, 42, and 46 °C. These $I(q)$'s were obtained by circularly averaging two dimensional data of scattered intensity. The incoherent scattered intensity was obtained to be $I_{inc} = 0.0871$ cm^{-1} for NIPA/AAc monomer solutions at the same concentration, which is comparable to the calculated value of 0.0316 cm^{-1}. Note that I_{inc} is negligibly smaller than $I(q)$'s. The solid lines indicate the fitted intensity functions with the fitting parameter sets of (χ, K) = (−0.221, 1.359), (0.322, 1.412), and (0.748, 1.021), respectively, for the gels at 26, 42, and 46 °C. It should be noted that K can be estimated by the following equation[25,26]

$$K = \frac{N_A}{v_B}\left[b_A\left(\frac{v_B}{v_A}\right) - b_B\right]^2 \tag{16}$$

where N_A is Avogadro's number, and v_i and b_i are the molar segment volume and the scattering length of component i, respectively. The value of K is estimated to be 0.51 cm^{-1} for NIPA/AAc gels with $\phi = 0.078$, where the value for component B was chosen to be the arithmetic average of those of the NIPA and AAc monomers. Therefore, the agreement of the fitted and calculated values of K is satisfactory, if one takes into account the experimental error of the absolute intensity calibration and the presence of preparation residue in the gel. The value a was fixed to be 8.12 Å[14,27] and other parameters were chosen to be those at preparation, i.e., $\phi = \phi_0 = 0.078$, $f = f_0 = 0.0457$, and $N = 40$. It should be noted that each of the observed $I(q)$'s was reproduced

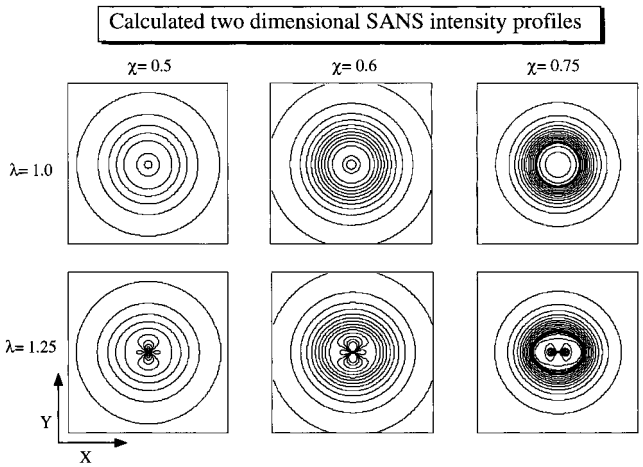

Figure 6. Calculated two dimensional SANS intensity profiles of weakly charged gels at $\chi = 0.5$, 0.6, and 0.75 for undeformed ($\lambda = 1.0$) (upper) and deformed gels ($\lambda = 1.25$) (lower). The scattering direction is parallel to the y axis.

by floating only two parameters, i.e., χ and K. Although some deviations are seen at low q's, the theory well reproduces the peak position and the global profile. The estimated value of χ (=−0.221) for the data at 26 °C seems to be inappropriate since χ should be positive even at this temperature. This contradiction results from the fact that the theory breaks down for the good solvent regime. Thus, by restricting the analysis being only in the poor solvent regime, we reproduced a two-dimensional scattering intensity profile by using the χ parameter estimated here.

Figure 6 shows a series of 2D scattering intensity profiles for weakly charged polymer gels. Patterns in the upper column show those for undeformed gels (i.e., $\lambda = 1.0$) and the bottom patterns correspond to those at $\lambda \equiv \lambda_y = 1.25$. It can be said, by comparing Figure 6 with Figure 3, that the scattering intensity patterns are well reproduced by the theory at least qualitatively. A more careful comparison leads to the following facts: (1) Regarding Figure 3a and the case where $\chi = 0.5$, it can be understood that either the predicted anisotropy is too small to be detected by experiment or the value of χ in the theoretical calculation is overestimated. (2) In Figure 3b and in the case where $\chi = 0.6$, both show the so-called abnormal butterfly patterns in the deformed gels. (3) The elliptic pattern at 46 °C is well reproduced by the theory.

Figure 7 shows the observed scattered intensities of NIPA/AAc gel observed at 46 °C with (a) $\lambda = 1.07$ and with (b) $\lambda = 1.25$, in the x (open squares) and y (open circles) directions, respectively, which are obtained by taking a sector average with 20°. In the case of $\lambda = 1.07$, the anisotropy in $I(q)$'s is not so large because of a low deformation ratio. The solid curves indicate fitted intensity functions with the RP theory, where three parameters, i.e., the scaling factor, K, the interaction parameter, χ, and the deformation ratio, λ, were floated. As shown in the figure, the fitting was satisfactory. On the other hand, the highly anisotropic scattered patterns for the case of $\lambda = 1.25$, shown in Figure 7b, were also nicely fitted with the theory.

Figure 8 shows the result of fitted values of λ (filled symbols) as a function of the macroscopic deformation, Δx. Open symbols denote the values of λ determined by the peak position in $I(q)$. Though there are some deviations in the y direction, a good agreement between

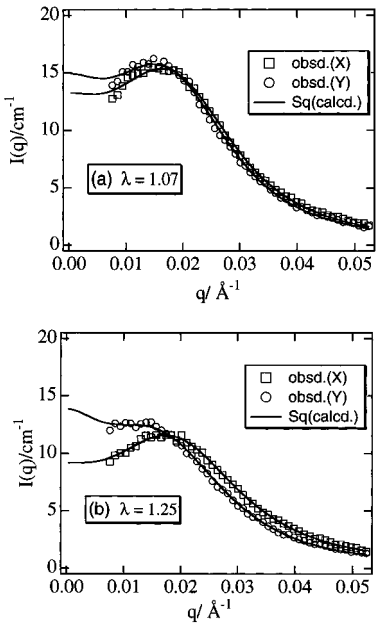

Figure 7. Observed scattered intensity functions at (a) $\lambda = 1.07$ and (b) $\lambda = 1.25$, along the x (the normal; squares) and the y (the stretching; circles) directions, respectively.

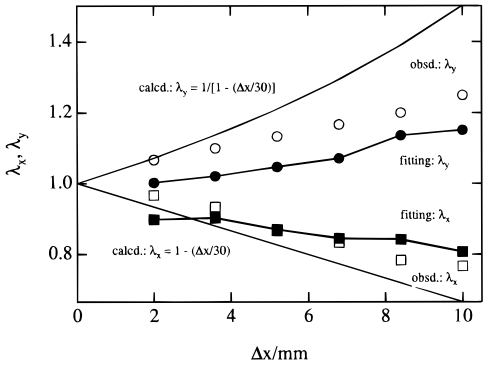

Figure 8. Variation of the fitted λ's as a function of deformation of the gel, Δx. See Figure 4 for comparison.

the observed and fitted values of λ is obtained in the x direction. Because χ is a thermodynamic quantity, it should not depend on the degree of deformation λ. Similarly, K should be constant irrespective of temperature and λ. The values of fitted χ and K were in the ranges 0.73−0.76 and 1.0−1.4 irrespective of the direction and the degree of deformation. Although the fitted values are scattered, these values seem to be within the allowance.

3. Static Inhomogeneities vs Thermal Fluctuations. Parts a−c of Figure 9 show the calculated SANS structure factors, $S(q)$, $C(q)$, and $G(q)$, for weakly charged gels with $\phi = \phi_0 = 0.078$ and $f = f_0 = 0.0457$, along the equator (left) and the meridian (right). At $\chi = 0.5$, $C(q)$ is stronger in the y direction than in the x direction, indicating the abnormal butterfly pattern although the intensity is much lower than in the cases of $\chi = 0.6$ and $\chi = 0.75$. For $\chi = 0.6$, a scattering maximum appears in both directions and the trend of the butterfly pattern is still preserved (i.e., an upturn of $C(q)$ in the low q region in the y direction). This tendency becomes more prominent for $\chi = 0.75$. Note that the difference in $G(q)$ in the two directions is always much smaller than that in $C(q)$ as far as the value of χ is the same. Therefore, the theory predicts that the effect of deformation results in strong anisotropy in $C(q)$

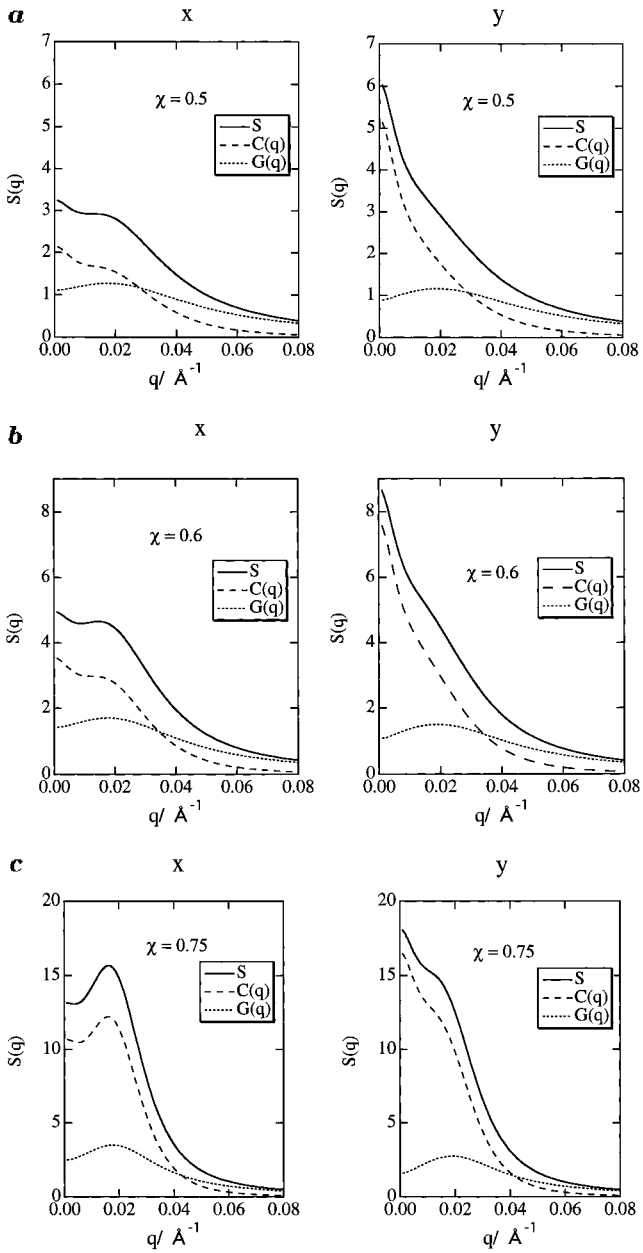

Figure 9. Calculated structure factor, $S(q)$, and the contributions of the static inhomogeneities, $C(q)$, and the dynamic fluctuations, $G(q)$, for (a) $\chi = 0.5$, (b) $\chi = 0.6$, and (c) $\chi = 0.75$.

but not in $G(q)$. This conclusion may be reasonable if one considers the origins of $C(q)$ and $G(q)$ being the static inhomogeneity and the thermal fluctuations, respectively.

Another interesting feature of anisotropic scattering is expected by further increasing χ. Figure 10 shows calculated SANS structure factors, $S(q)$, $C(q)$, and $G(q)$ for a weakly charged gel calculated with the same parameter as discussed in Figure 9, while χ is set to be 0.8. This figure clearly shows a crossover of $S(q)$; $S(q_{m,x}) > S(q_{m,y})$. This indicates that a more organized structure is preferentially formed along the x direction. Experimental verification of such a scattering pattern predicted by the theory could not be conducted because the scattered intensity at $T \geq 46$ °C exceeded the limitation of the detector.

As disclosed in this study, the structure factor of weakly charged polymer gels are successfully recovered by the Rabin−Panyukov theory. However, it should be

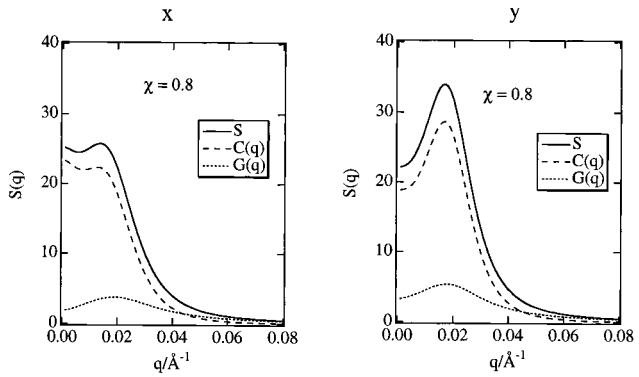

Figure 10. Calculated structure factor, $S(q)$, and the contributions of the static inhomogeneities, $C(q)$, and the dynamic fluctuations, $G(q)$, for $\chi = 0.8$.

noted that the gels studied here were prepared by redox polymerization from a monomer solution of NIPA/AAc in the presence of cross-links. On the other hand, the theory assumes a spontaneously cross-linked polymer network. Such gels can be prepared by γ-ray irradiation of polymer solutions. In the case of the former, a more inhomogeneous structure is expected because the differences in (1) the monomer reaction ratios among NIPA, AAc, and the cross-linker and (2) diffusion of monomers to participate in polymerization and/or cross-linking affect the monomer sequence of the product polymer network. In spite of such ambiguities, the experimental results were well reproduced by the theory. This may suggest a universality of the gel structure, namely a gel being matter with frozen inhomogeneities and thermal concentration fluctuations. A decomposition of the observed scattered intensity into the static inhomogeneity and the thermal fluctuations by dynamic light scattering, which was successfully employed elsewhere,[13] may provide a clear evidence of the origin of the scattering maximum observed for weakly charged gel. A preliminary experiment on a series of γ-ray cross-linked polymer gels, however, suggests that the γ-ray cross-linked gels seem to be more inhomogeneous than those prepared by redox polymerization. Analysis along this line is on progress.

Conclusion

Small-angle neutron scattering experiments have been conducted on weakly charged gels of poly(*N*-isopropylacrylamide-*co*-acrylic acid) (NIPA/AAc) as a function of temperature, T, and degree of uniaxial deformation λ. At 26 °C, where the solvent (i.e., water) is not a poor solvent, no noticeable effect by deformation was observed. This is explained by a relatively large contribution of the thermal fluctuations with respect to the static inhomogeneity. At 42 °C, where $\chi \approx 0.6$, the so-called abnormal butterfly pattern appeared for $\lambda = 1.25$. This results from an lowering of osmotic pressure which allows the gel to fluctuate more easily than the case at 26 °C. By a further increase in the temperature to 46 °C, a distinct scattering maximum appeared, i.e., a circular-shell pattern for undeformed gel and an elliptic-shell pattern for deformed gels. The elliptic-shell pattern of SANS intensity was well reproduced by the Rabin−Panyukov theory for weakly charged gels.

Acknowledgment. This work is partially supported by the Ministry of Education, Science, Sports and Culture, Japan (Grant-in-Aid, Nos. 08231245 and 09450362 to M.S.). F.I. acknowledges the Research Fellowship of the Japan Society for the Promotion of Science for Young Scientists. The authors are grateful to Y. Rabin and Y. Shiwa for helpful discussions.

References and Notes

(1) Bastide, J.; Leibler, L. *Macromolecules* **1988**, *21*, 2647.
(2) Baumgartner, A.; Picot, C. E. In *Molecular Basis of Polymer Networks*; Baumgartner, A., Picot, C. E., Ed.; Springer: Berlin, 1989.
(3) Pusey, P. N.; van Megen, W. *Physica A* **1989**, *157*, 705.
(4) Onuki, A. *J. Phys. II Fr.* **1992**, *2*, 45.
(5) Rouf, C.; Bastide, J.; Pujol, J. M.; Schosseler, F.; Munch, J. P. *Phys. Rev. Lett.* **1994**, *73*, 830.
(6) Panyukov, S.; Rabin, Y. *Phys. Rep.* **1996**, *269*, 1.
(7) Bastide, J.; Candau, S. J. In *Structure of Gels as Investigated by Means of Static Scattering Techniques*; Bastide, J., Candau, S. J., Ed.; John Wiley: New York, 1996; Chapter 9, p 143.
(8) Shibayama, M. *Macromol. Chem. Phys.* **1998**, *198*, 1.
(9) Mendes, E.; Oeser, R.; Hayes, C.; Boue, F.; Bastide, J. *Macromolecules* **1996**, *29*, 5574.
(10) Mendes, E. J.; Lindner, P.; Buzier, M.; Boue, F.; Bastide, J. *Phys. Rev. Lett.* **1991**, *66*, 1595.
(11) Onuki, A. *Adv. Polym. Sci.* **1993**, *109*, 63.
(12) Shibayama, M.; Fujikawa, Y.; Nomura, S. *Macromolecules* **1996**, *29*, 6535.
(13) Shibayama, M.; Takata, T.; Norisuye, T. *Physica A* **1998**.
(14) Shibayama, M.; Tanaka, T.; Han, C. C. *J. Chem. Phys.* **1992**, *97*, 6842.
(15) Shibayama, M.; Ikkai, F.; Inamoto, S.; Nomura, S.; Han, C. C. *J. Chem. Phys.* **1996**, *105*, 4358.
(16) Borue, V.; Erukhimovich, I. *Macromolecules* **1988**, *21*, 3240.
(17) Schosseler, F.; Moussaid, A.; Munch, J. P.; Candau, S. J. *Macromolecules* **1991**, *24*, 225.
(18) Shibayama, M.; Tanaka, T. *J. Chem. Phys.* **1995**, *102*, 9392.
(19) Rabin, Y.; Panyukov, S. *Macromolecules* **1997**, *30*, 301.
(20) Shibayama, M.; Kawakubo, K.; Norisuye, T. *Macromolecules* **1998**, *31*, 1608.
(21) Mendes, E.; Schosseler, F.; Isel, F.; F., B.; Bastide, J.; Candau, S. J. *Europhys. Lett.* **1995**, *32*, 273.
(22) Geissler, E.; Duplessix, R.; Hecht, A. M. *Macromolecules* **1983**, *16*, 712.
(23) Flory, P. J. *Principles in Polymer Chemistry*; Cornell Univ.: Ithaca, NY, 1953.
(24) Tanaka, T. *Phys. Rev. Lett.* **1978**, *40*, 820.
(25) Shibayama, M.; Yang, H.; Stein, R. S.; Han, C. C. *Macromolecules* **1985**, *18*, 2179.
(26) Higgins, J. S.; Benoit, H. C. *Polymers and Neutron Scattering*; Clarendon Press: Oxford, England, 1994.
(27) Kubota, K.; Fujishige, S.; Ando, I. *Polym. J.* **1990**, *22*, 15.

MA971411B